Electronic Supplementary Material (ESI) for Nanoscale Advances.


## Electronic Supplementary Information

# Direction- and polarization-tunable spontaneous emission beneficial from diffraction orders of square R6G-nanopore array

Shijia He,[a,b] Yi Wang,*[a,b] Tianyu Wang,[b] Dongda Wu,[a,b] Junqiao La,[a,b] Jiang Hu,[b] Jiamin Xiao [b] and Wenxin Wang*[a,b]

[a.] *College of Physics and Optoelectronic Engineering, Harbin Engineering University, 150001 Harbin, China*

[b.] *Qingdao Innovation and Development Center of Harbin Engineering University, Harbin Engineering University, 266500 Qingdao, China*

### Corresponding Authors

*Email: yi.wang@hrbeu.edu.cn, wenxin.wang@hrbeu.edu.cn

## 1. The liquid-encapsulated manner of anodic aluminum oxide (AAO) membrane combined with rhodamine 6G (R6G) aqueous solution

The AAO membrane is surrounded by the R6G aqueous solution in a liquid-encapsulated manner. The R6G aqueous solution is evenly distributed on the surface of AAO membrane by dropwise addition. Then a coverslip is placed on its surface to completely immerse the AAO in R6G aqueous solution. As shown in Fig. S1a, the AAO membrane and R6G aqueous solution are packaged between the bottom glass slide and the cover glass in the form of liquid encapsulation. The emission direction of R6G can be regulated by the microscopic structure of the square lattice, which is presented in Fig. S1b.

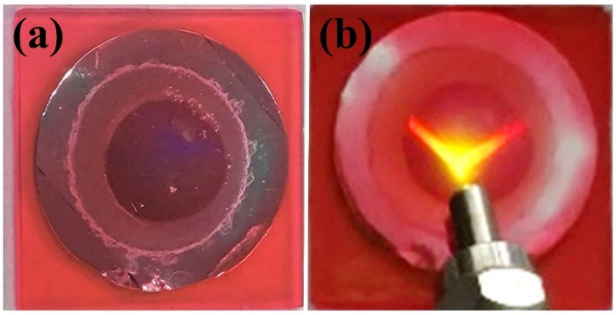


**Fig. S1** Packaging AAO membrane with R6G. (a) Photo of the AAO membrane immersed in R6G aqueous solution in the glass capsule. (b) Photo of R6G emission propagation on the AAO membrane of square lattice.

## 2. Photoluminescence (PL) comparison of R6G on Al foil and AAO membrane

Under the driving light of 532 nm, the difference of R6G emission spectra on Al foil and AAO membrane are shown in Fig. S2. The PL of R6G on the Al foil is isotropic at different emission angles in Fig. S2a, but the R6G emission on the AAO membrane shows directionality when the Γ point energy of AAO overlap with the dominant PL emission wavelength of R6G (560 nm) exactly (Fig. S2b). Its PL intensity enhancement shows specific angle-dependent properties as the emission angle changes from 0° to 30° (Fig. S2b). The directional emissions are observed to be related to the diffraction orders (DOs) of lattice arrangement.

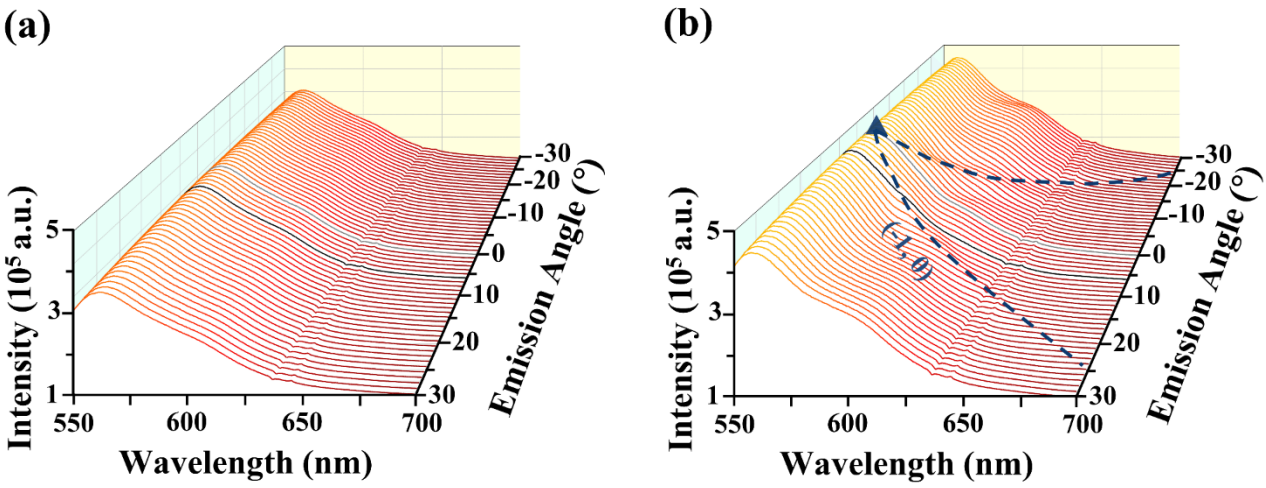


**Fig. S2** The PL of R6G on (a) Al foil and (b) AAO membrane under excitation of 532 nm laser at the incident angle of 40°, wherein the gray solid lines and black solid lines are the spectra at emission angles of 0° and 6°, respectively. The blue dotted lines represent the variation tendency of (-1, 0) mode from -30° to 30°.

## 3. The polarization of square lattice at Γ point under a white light source

By using a white light source, a 45° polarization reflection can be observed at Γ point (560 nm), as shown in Fig. S3. The Polarization is closely related to the lattice symmetry.

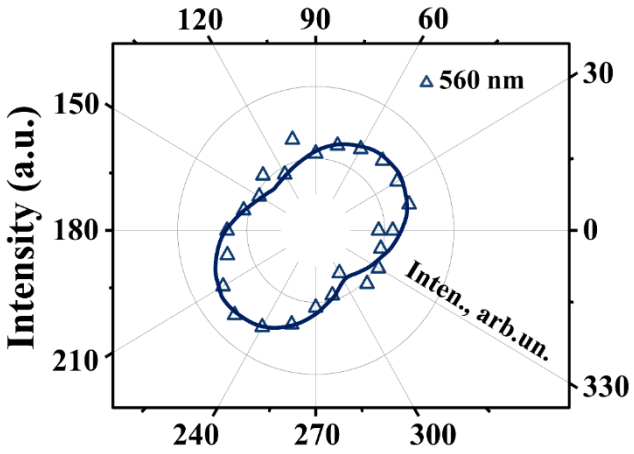


**Fig. S3** The polarization of Γ point under white light source. The blue triangles indicate the intensity of reflection spectra at 560 nm with different polarization angle, and the solid blue line is the fitting curve.

## 4. The polarization degree comparison between the PL emission of 90° polarization dissimilarity

The PL emission behaves horizonal-polarization dependent ($\vartheta_p$ = 0°) and vertical-polarization dependent ($\vartheta_p$ = 90°) as it couples to the (0, ±1) mode and (-1, 0) mode, respectively. Except the polarization directions, the degree of polarization (DoP) between the two signals are different as well. DoP can be expressed as the ratio of the difference to the sum of the light intensities between the two mutually perpendicular axes. It defined as $P = (I_{max} - I_{min})/(I_{max} + I_{min})$,[1] where $I_{max}$ and $I_{min}$ are the maximum and minimum light intensities within all the spectra of different angles. According to the two kinds of polarization dependent signals in Fig. S4a and Fig. S4b, the corresponding $I_{max}$ and $I_{min}$ can be extracted as the length of the long arrow and short arrow at 554 nm and 582 nm, respectively. The PL emission exhibits a horizontal polarization correlation with DoP of 77% ($\vartheta_p$ = 0°, Fig. S4a) when it coupled with (0, ±1) mode, and a vertical polarization correlation with DoP of 43% ($\vartheta_p$ = 90°, Fig. S4b) when it coupled with the (-1, 0) mode.

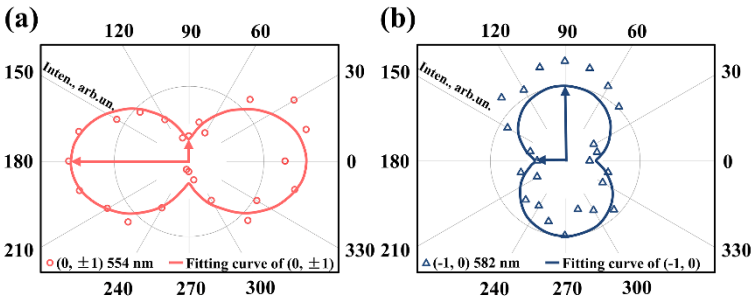


**Fig. S4** The off-angle SE (6°) of R6G as a function of polarization at (a) 554 nm and (b) 582 nm, respectively. The long arrow and short arrow represent the corresponding light intensities at polarization direction of 0° (red) and 90° (blue), respectively.

## 5. Regulation of 90° difference polarization by DOs of AAO membrane under white light source

At the 6° off-angle condition, the reflection of AAO membrane under white light source present the same polarization with the emission of R6G, as shown in Fig. S5. The 0° and 90° polarization correspond to the DOs of (0, ±1) and (-1, 0), respectively, which further illustrates the polarization dependence on DOs.

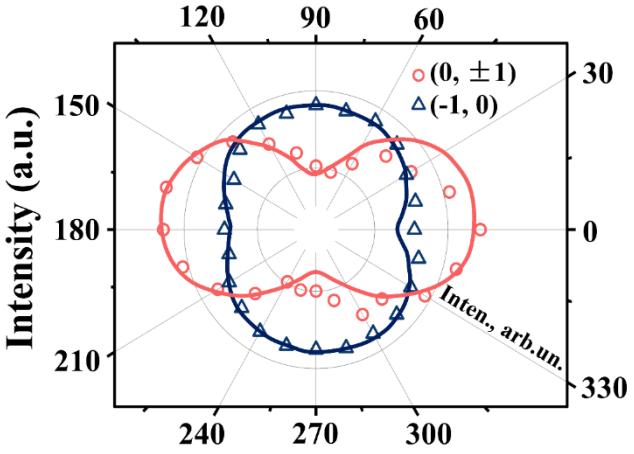


**Fig. S5** A 90° difference polarization of reflection spectra at (0, ±1) and (-1, 0) DOs with a white light source. The red circles and blue triangles represent the reflection intensity at (0, ±1) and (-1, 0) DOs, the corresponding wavelength is 554 nm and 582 nm, respectively, the red solid line and blue solid line are their fitting curves.

## 6. The schematic optical path of the Fourier image system

A homemade polarized momentum space imaging system was constructed with incident light emitted from a laser (560 nm) and focused onto the sample through an objective lens (MXPLFLN50X, 50×, NA 0.8), which is used to exhibit the light propagation in reciprocal space and to further explain the underlying physics of Fourier image. The schematic optical path is illustrated in Fig. S6. The back focal plane of the same objective is imaged to a two-dimensional charge-coupled device (CCD) camera (Zeiss Axio Cam ERc 5s Rev. 2.0) using a series of convex lenses. The information carried by the back focal plane of the objective lens corresponds to the Fourier space information. The polarizer is placed on the focal plane of the lens 1 ($L_1$) to adjust the polarization, and the aperture is placed next to it.

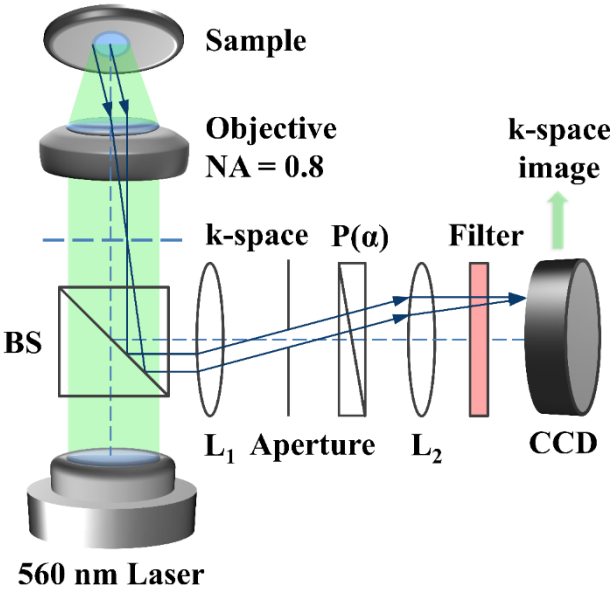


**Fig. S6** The schematic optical path of the Fourier image system, wherein BS represents beam splitter, L is lens, and P is polarizer.

## 7. The SEM images of AAO membranes with different pore diameters

The diameter of the unit cell is a critical determinant for varying the resonant energy of the DOs. Through the chemical wet etching in 5 wt% phosphoric acid with a water bath of 55 ℃, the 110 nm initial diameter of AAO membrane can be expanded to 330 nm. In addition, different pore diameters can be achieved by regulating the pore-expanding time. SEM images in Fig. S7 present the pore diameter changing process. The pore diameters of samples are 110 nm, 150 nm, 185 nm, 200 nm, 220 nm, 240 nm, 300 nm, and 330 nm, and the corresponding pore-expanding time are 0 min, 2 min, 4 min, 6 min, 8 min, 10 min, 12 min and 14 min, respectively.

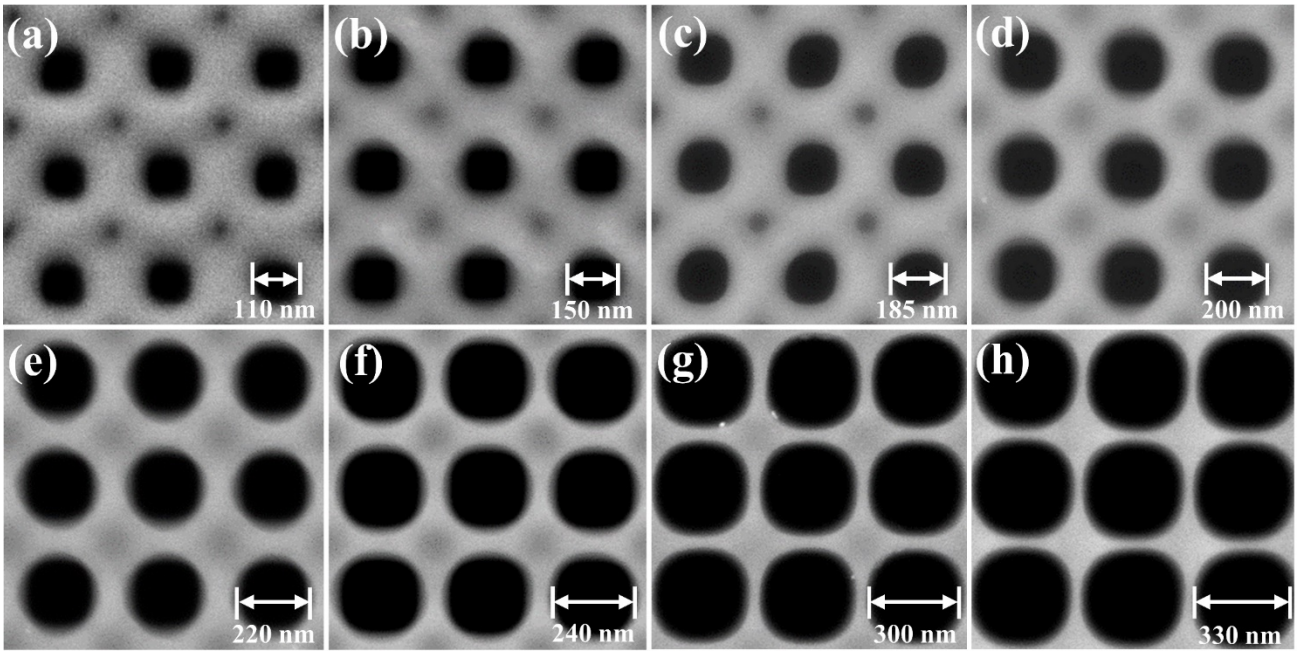


**Fig. S7** The SEM images of AAO membranes with pore diameters of (a) 110 nm, (b) 150 nm, (c) 185 nm, (d) 200 nm, (e) 220 nm, (f) 240 nm, (g) 300 nm and (h) 330 nm, respectively.

## 8. Experimental reflection dispersion of AAO membranes with different pore diameters

Reflection dispersion of AAO membranes with different pore diameters in aqueous solution (refractive index of 1.33) are performed under a white light source in Fig. S8. The Γ point energy can be extended into a flexible spectral range from 1.99 eV to 2.51 eV, where the energy of Γ point increasing with the pore diameter.

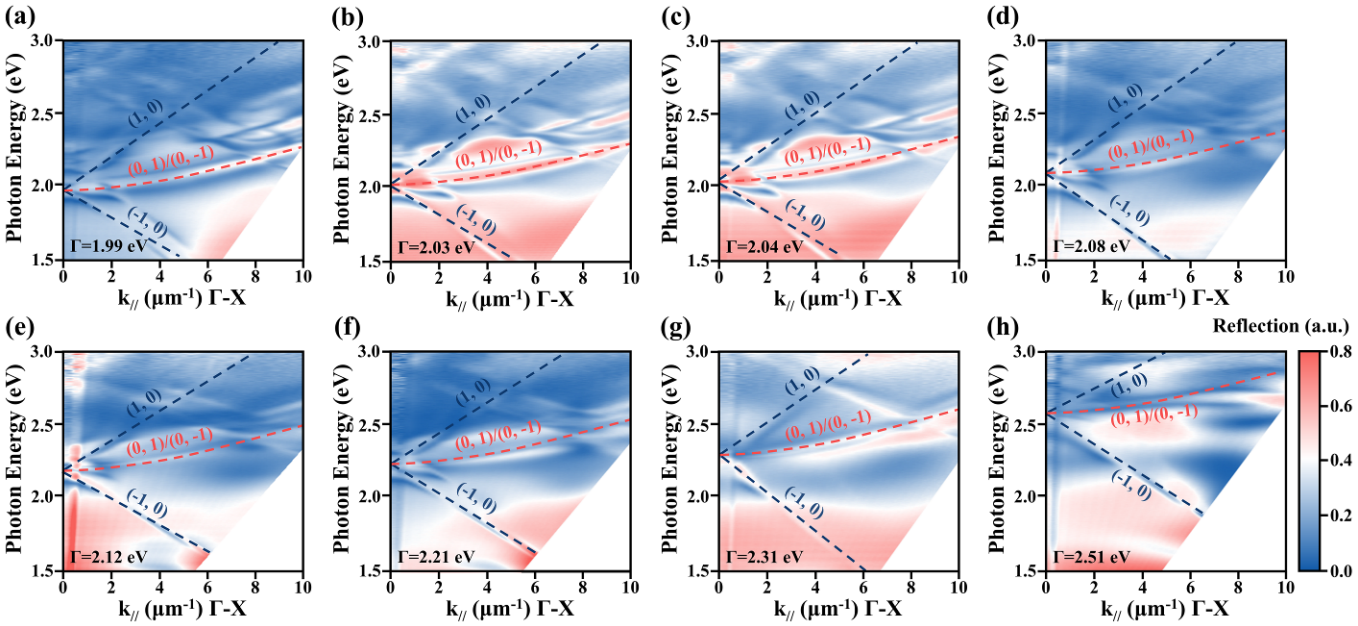


**Fig. S8** E-$k_{//}$ dispersion of AAO membranes with pore diameters of (a) 110 nm, (b) 150 nm, (c) 185 nm, (d) 200 nm, (e) 220 nm, (f) 240 nm, (g) 300 nm and (h) 330 nm, the corresponding energy of Γ point are marked at the left bottom, respectively.

## 9. Simulated reflection dispersion of AAO membranes with different pore diameters

Finite-different time-domain (FDTD) method is used to simulate the reflection dispersion of AAO membranes in aqueous solution (refractive index of 1.33), as shown in Fig. S9, in which the pore diameters are 110 nm, 185 nm, 220 nm and 300 nm. The simulated results possess the same trend with the measured dispersions.

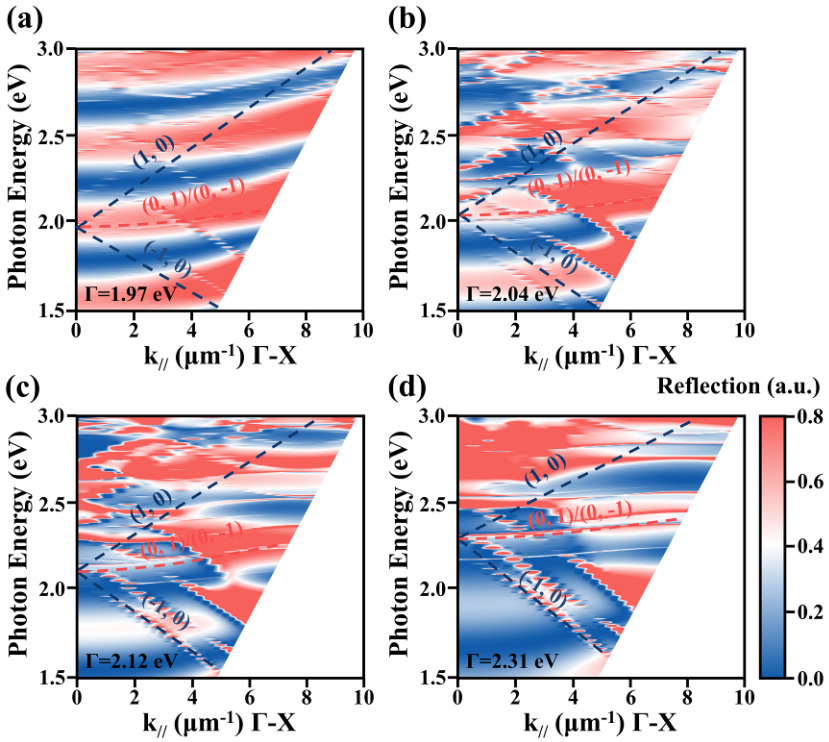


**Fig. S9** Simulated reflection dispersion of AAO membranes with pore diameters of (a) 110 nm, (b) 185 nm, (c) 220 nm and (d) 300 nm, respectively.

## 10. Correspondence between SE of R6G and DOs of AAO membranes

Under the driving light of 532 nm, the directionality of R6G emission on the AAO membrane are shown in Fig. S10. The variation tendency of the dominant emission wavelength of R6G is well consistent with DOs of AAO membrane, exhibiting the modulation effect of square lattice on the SE of R6G.

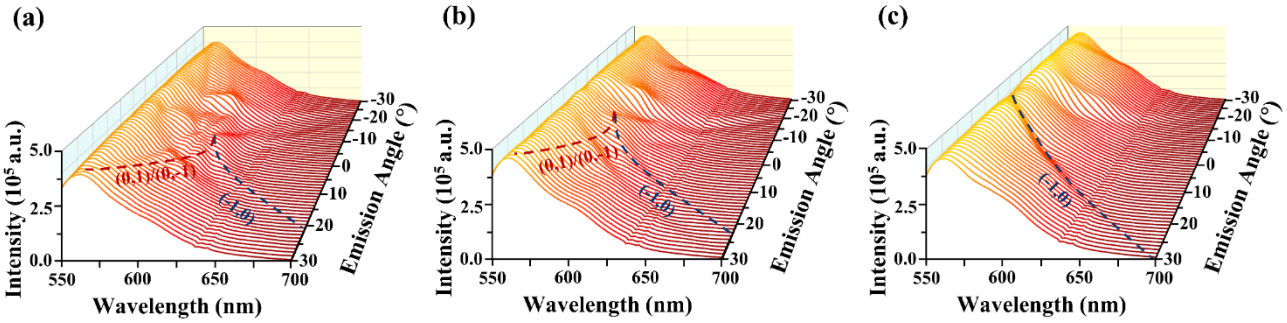


**Fig. S10** Correspondence between SE of R6G and DOs of AAO membranes, the pore diameters are (a) 185 nm, (b) 220 nm and (c) 300 nm, respectively.

## 11. Polarization regulation of AAO membrane at specific wavelength under white light source

Polarization of reflected light are measured under a white light source. Here, DOs of (0, ±1) and (-1, 0) are located at 560 nm, the corresponding emission angle is 23° and 5°, respectively. As shown in Fig. S11, the reflected light exhibits horizonal-polarization dependent with (0, ±1) modes and vertical polarization dependence with (-1, 0) mode, achieving a 90° difference polarization at a specific wavelength and indicating the polarization dependence of different DOs.

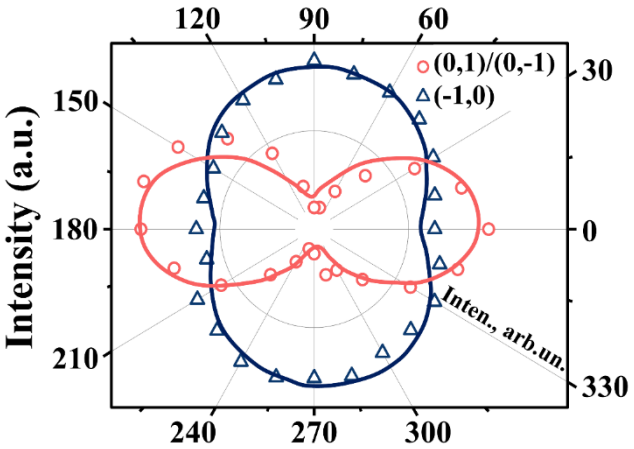


**Fig. S11** Polarization of reflected light at wavelength of 560 nm under white light source. The red circle and blue triangle represent the intensity of (0, ±1) and (-1, 0) DOs at wavelength of 560 nm, the red solid line and blue solid line are their fitting curves, respectively.

## References

1 B. DeBoo, J. Sasian and R. Chipman, *Opt. Express*, 2004, **12**, 4941-4958.